

# Magnetic and nonmagnetic phases in doped $AB_2 t$ - $J$ Hubbard chains

R. R. Montenegro-Filho and M. D. Coutinho-Filho

*Laboratório de Física Teórica e Computacional, Departamento de Física, Universidade Federal de Pernambuco, 50670-901, Recife-PE, Brazil*

(Received 11 May 2014; revised manuscript received 18 July 2014; published 11 September 2014)

We discuss the rich phase diagram of doped  $AB_2 t$ - $J$  chains by using data from density matrix renormalization group and exact diagonalization techniques. The  $J$  vs  $\delta$  (hole doping) phase diagram exhibits regions of itinerant ferrimagnetism, incommensurate, resonating valence bond and Nagaoka states, phase separation, and Luttinger liquid (LL) physics. Several features are highlighted, such as the modulated ferrimagnetic structure, the occurrence of Nagaoka spin polarons in the underdoped regime and small values of  $J = 4t^2/U$ , where  $t$  is the first-neighbor hopping amplitude and  $U$  is the on-site repulsive Coulomb interaction, incommensurate structures with nonzero magnetization, and strong-coupling LL physics in the high-doped regime. We also verify that relevant findings are in agreement with the corresponding findings in square and  $n$ -leg ladder lattices. In particular, we mention the instability of Nagaoka ferromagnetism against  $J$  and  $\delta$ .

DOI: [10.1103/PhysRevB.90.115123](https://doi.org/10.1103/PhysRevB.90.115123)

PACS number(s): 71.10.Fd, 71.27.+a

## I. INTRODUCTION

The  $t$ - $J$  version of the Hubbard Hamiltonian [1] is a key model for understanding strongly correlated electron systems. The model is defined through only two *competing* parameters: the hopping integral  $t$ , which measures the electron delocalization through the lattice, and the exchange coupling  $J = 4t^2/U$ , where  $U \gg t$  is the on-site Coulomb repulsion. In fact, several versions of the simplest Hubbard Hamiltonian, with a single orbital at each lattice and the on-site Coulomb repulsion, have been extensively used to model a variety of phenomena, such as the metal-insulator transition [2], quantum magnetism [3] and high- $T_c$  superconductivity [4]. Moreover, exact solutions [1] and rigorous results [5,6] have played a central role in this endeavor.

We emphasize Lieb's theorem [7], a generalization of the one by Lieb and Mattis [8] for Heisenberg systems, which asserts that the ground state (GS) total spin of a bipartite lattice at half filling and  $U > 0$  is given by  $S_{GS} = |N_A - N_B|/2$ , where  $N_A$  ( $N_B$ ) is the number of sites on sublattice  $A$  ( $B$ ); indeed, Lieb's theorem has greatly enhanced the investigation of new aspects of quantum magnetism [6]. In particular, we mention the occurrence of *ferrimagnetic* GS, in which case we select studies using Hubbard or  $t$ - $J$  models [9–15], including the Heisenberg strong-coupling limit [16–18], on chains with  $AB_2$  or  $ABC$  topological structures with  $S_{GS} = 1/2$  per unit cell [9–13,16,17], which implies ferromagnetic and antiferromagnetic long-range order [10]. Further, the inclusion of competing interactions or geometrical and kinetic frustration [19–21] enlarges the classes of models, thereby allowing ground states not obeying Lieb or Lieb and Mattis theorems. These studies have proved effective in describing magnetic and other physical properties of a variety of organic, organometallic, and inorganic quasi-one-dimensional compounds [19,22].

Of particular physical interest are doped systems, although in this case rigorous results are much rarer [6]. One exception is Nagaoka's theorem [23], which asserts that for  $J = 0$  ( $U \rightarrow \infty$ ) the  $t$ - $J$  model with one hole added to the undoped system (half-filled band) is a *fully polarized ferromagnet*, favored

by the hole kinematics, if the lattice satisfies the so-called connectivity condition [24]. A long-standing problem about this issue is the stability of the ferromagnetic state for finite hole densities and finite values of  $J$ . Numerical results have indicated [25,26] that two-dimensional lattices display a fully polarized GS for  $J = 0$  and  $\delta \lesssim 0.2$ , where  $\delta = N_h/N$ , with  $N_h$  ( $N$ ) the total number of holes (sites), while analytical studies [27,28] have suggested that this state is stable up to  $J_t \sim \delta^2$ .

Further, a ubiquitous phenomenon in doped strongly correlated materials is the occurrence of inhomogeneous states, particularly spatial *phase separation* in nano- and mesoscopic scales [29] and *incommensurate* states [29,30]. In underdoped high- $T_c$  materials, dynamical and static stripes in copper oxide planes have been the focus of intensive research [31]. Concerning two-dimensional  $t$ - $J$  or Hubbard models, phase separation into hole-rich and no-hole regions was discussed in the large- and small- $J$  limits [32]. However the precise charge distribution in the ground state remains controversial. The use of distinct and refined numerical methods has pointed to striped [33] or uniform phases [34]; recently, it was claimed that the origin of this issue relies on the strong competition between these phases [35]. For the linear  $t$ - $J$  Hubbard chain the physics is more clear [36], and phase separation takes place for  $J = 2.5$  to  $3.0$ , depending on the doping value, but it is absent in the small- $J$  regime.

In this work, we use density matrix renormalization group (DMRG) [37] techniques and Lanczos exact diagonalization (ED) to obtain the ground-state phase diagram and the low-energy-excitation properties of the doped  $t$ - $J$  model on  $AB_2$  chains [9] for  $J = 0.0$  to  $0.4$ . We verify the occurrence of an itinerant modulated ferrimagnetic (FERRI) phase in the underdoped regime, regions of incommensurate (IC) states and Nagaoka ferromagnetism (F), and two regions of phase separation (PS), in which IC and F states coexist with the resonating valence bond state (RVB), respectively. In addition, we find that the RVB state is the stable phase at  $\delta = 1/3$  and identify a crossover region that ends at the onset of a Luttinger liquid (LL) phase at  $\delta = 2/3$ , above which the LL physics [38] sets in.

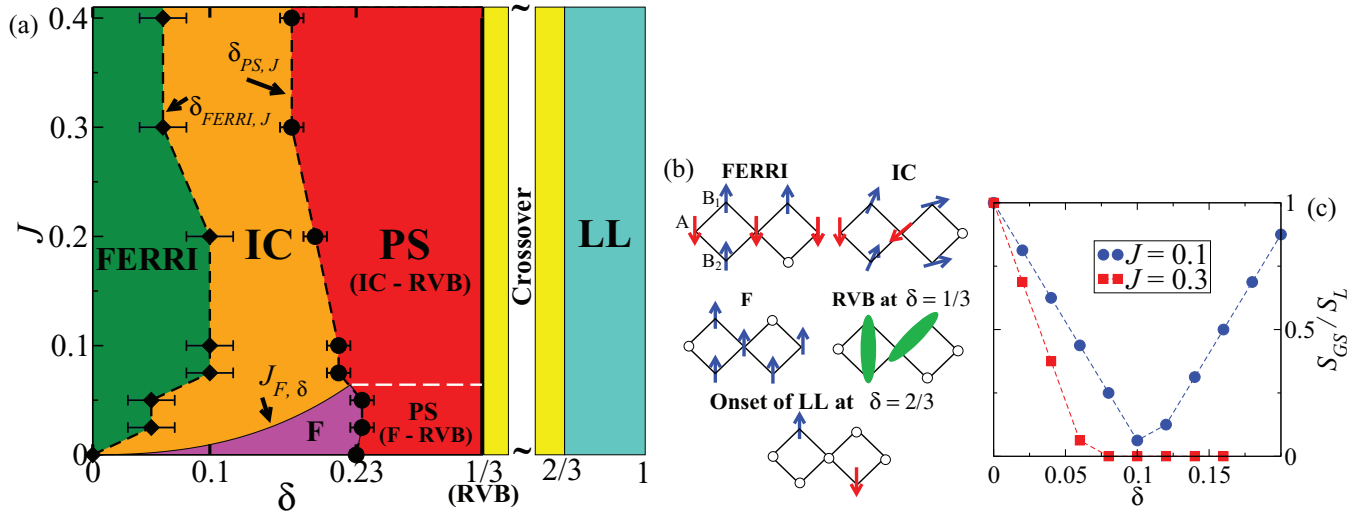


FIG. 1. (Color online) (a) GS phase diagram for the  $AB_2 t$ - $J$  model (error bars account for the discrete values assumed by  $\delta$  in a finite-size system). The phases are illustrated in panel (b): modulated ferrimagnetism (FERRI), incommensurate (IC), Nagaoka ferromagnetism (F), short-range resonating valence bond (RVB) states, phase separation (PS), and Luttinger liquid (LL). The estimated transition lines  $\delta_{FERRI,J}$ ,  $\delta_{PS,J}$ , and  $J_{F,\delta}$  are also pointed out. (c) Ground-state total spin  $S_{GS}$  is normalized by its value in the undoped regime:  $S_L \equiv (N_c/2) - 0.5$ , as function of  $\delta$  for the indicated values of  $J$  and  $N = 3N_c + 1 = 100$ .

## II. PHASE DIAGRAM

The  $t$ - $J$  model reads

$$H_{t-J} = -t \sum_{(i,j),\sigma} P_G (c_{i\sigma}^\dagger c_{j\sigma} + \text{H.c.}) P_G + J \sum_{(i,j)} \left( \mathbf{S}_i \cdot \mathbf{S}_j - \frac{1}{4} n_i n_j \right), \quad (1)$$

where  $c_{i\sigma}$  annihilates electrons of spin  $\sigma$  at site  $i$ ,  $n_i$  is the number operator at site  $i$ , and  $P_G = \prod_i (1 - n_{i\uparrow} n_{i\downarrow})$  is the Gutzwiller projector operator that excludes states with doubly occupied sites. In our simulations, we set  $t = 1$  and have considered chains with  $N_c$  ( $N$ ) unit cells (sites). In ED calculations, closed boundary conditions are used with  $N_c = 8$  ( $N = 3N_c$ ), while in the DMRG simulations open boundary conditions are used and the system sizes ranged from  $N_c = 33$  ( $N = 3N_c + 1 = 100$ ) to  $N_c = 121$  ( $N = 364$ ). We retain from 243 to 364 states in the DMRG calculations, and the typical discarded weight is  $1 \times 10^{-7}$ .

The ground-state (GS) phase diagram, shown in Fig. 1(a), displays the regions of the above-mentioned phases, illustrated in Fig. 1(b), including the estimated transition lines and the crossover region. A special feature of the  $AB_2$  chain is its symmetry [12,13,17] under the exchange of the labels of the  $B$  sites in a given unit cell  $l$  [identified in the FERRI state, Fig. 1(b)]. This symmetry implies a conserved parity  $p_l = \pm 1$  in each cell of the lattice. The phase diagram of a chain with  $N_c$  unit cells is calculated by obtaining the lowest energy for all subspaces with  $x$  contiguous cells of parity  $-1$  and the others  $N_c - x$  cells with parity  $+1$ , with  $x = 0, \dots, N_c$ , for fixed  $\delta$  and  $J$ . In the phase diagram shown in Fig. 1(a),  $p \equiv \sum_{i=1}^{N_c} p_i = +1$  for  $\delta \geq 1/3$ ,  $p \neq \pm 1$  in the PS region, and  $p = -1$  for  $\delta < \delta_{PS,J}$ . The magnetic configuration of a phase is identified by the total spin  $S_{GS}$ , local magnetization,

magnetic structure factor, and spin correlation functions. In what follows, we characterize the phases shown in Fig. 1(a).

## III. FERRIMAGNETISM AND TRANSITION TO IC STATES

At  $\delta = 0$  and  $J \neq 0$ , the *insulating* Lieb ferrimagnetic state with total spin quantum number  $S_{GS} = S_L \equiv N_c/2 - 0.5 \equiv S_L$  is found for a chain with open boundary conditions,  $N = 3N_c + 1 = 100$ , with an  $A$  site on each side. In order to evaluate the stability of this state against doping, we calculate  $S_{GS}$  as a function of  $\delta$  from the energy degeneracy in  $S^z$ . As shown in Fig. 1(c), as hole doping increases from  $\delta = 0$  to a critical value  $\delta = \delta_{FERRI,J}$ , the value of  $S_{GS}$  *decreases* linearly from  $S_L$  to 0 or to a residual value, signaling a smooth transition to the IC phase. However, for low-enough  $J$ ,  $S_{GS}$  of the IC phase *increases* linearly with  $\delta$  up to  $\delta = \delta_{PS,J}$ , the line at which PS occurs [see Fig. 1(a)], or up to the boundary,  $J_{F,\delta}$ , of the Nagaoka F phase. This unexpected behavior calls for an explanation.

In order to understand the behavior of  $S_{GS}$  for low  $J$  we have calculated the profiles of the magnetization,  $\langle S_l^z \rangle$ , in the spin sector  $S^z = S_{GS}$ , and of the hole density,  $\langle n_{h,l} \rangle$ , for  $J = 0.1$  (see Fig. 2). To help visualize the data, we use a linearized version of the lattice, as illustrated in Fig. 2(a). As shown in Fig. 2(b), for  $\delta = 0.04$  the holes distort the ferrimagnetic structure, which display a modulation with wavelength  $\lambda \approx 17$ , in antiphase with that exhibited by the hole (charge) density wave. We have thus identified a *modulated itinerant* ferrimagnetic phase in this underdoped regime. On the other hand, as shown in Fig. 2(c), for  $\delta = 0.18$  the magnetization has local maxima in coincidence with those of the hole-density profile. In this case, the IC phase is characterized by the presence of *ferromagnetic Nagaoka spin polarons* [28,39] due to a hole-density wave with  $\lambda \approx 4$ . Our results point to a value of  $J$  ( $\sim 0.2$ ) below which ferromagnetic ‘‘bubbles’’ appear as precursors of the F phase found for  $J < J_{F,\delta}$  [see Fig. 1(a)].

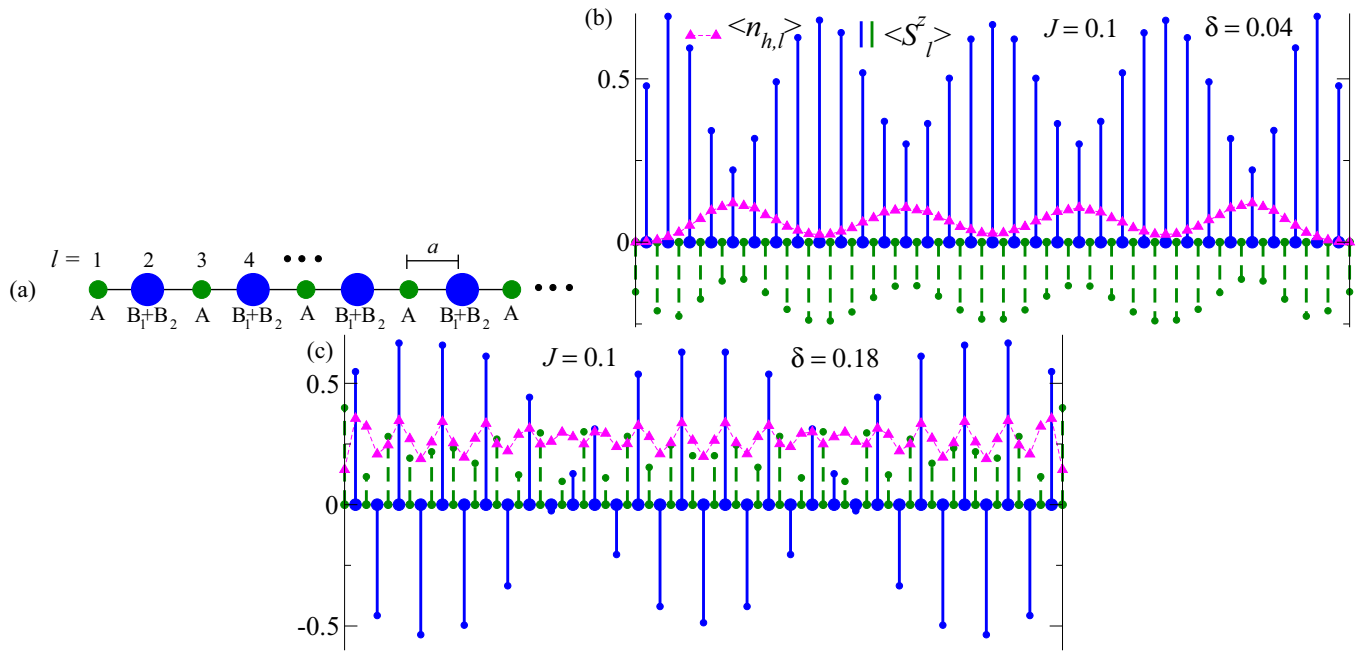


FIG. 2. (Color online) (a) Effective linear chain (spacing  $a \equiv 1$ ) associated with  $N = 3N_c + 1 = 100$  sites for  $J = 0.1$  used to illustrate the hole,  $\langle n_{h,l} \rangle$ , and spin,  $\langle S_l^z \rangle$ , profiles. (b)  $\delta = 4/100$  (FERRI phase) and (c)  $\delta = 18/100$  (IC phase).

For  $J = 0.3$ ,  $S_{GS} = 0$  in the IC phase, as shown in Fig. 1(c). In Figs. 3(a) and 3(b) we present the magnetic structure factor

$$S(q) = \frac{1}{S_L(S_L + 1)} \sum_{l,m} e^{iq(l-m)} \langle \mathbf{S}_l \cdot \mathbf{S}_m \rangle, \quad (2)$$

where  $l, m$ , and  $\mathbf{S}$  refer to the lattice representation shown in Fig. 2(a), for this value of  $J$  and doping ranging from  $\delta = 0$  up to  $\delta = 0.12$ . In a long-range-ordered ferrimagnetic state, sharp maxima at  $q = 0$  (ferromagnetism) and  $q = \pi$  (antiferromagnetism) are observed in the curve  $S(q)$  for  $\delta = 0$ . Adding two holes to the undoped state, sharp maxima at  $q = 0$  and  $\pi$  are also observed, while broad maxima occur for  $\delta = 0.04$ , indicating short-range ferrimagnetic order which evolves to the IC phase by increasing doping, before phase separation (IC-RVB) at the line  $\delta = \delta_{PS,J}$  [see Fig. 1(a)]. In the inset of Fig. 3(b) we show the departure of the maximum of  $S(q)$  from  $q = \pi$ .

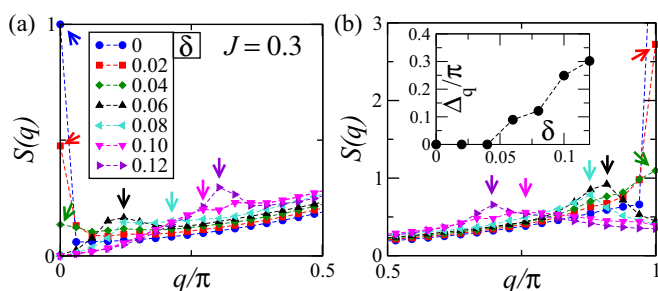


FIG. 3. (Color online) Chain with  $N = 3N_c + 1 = 100$  and  $J = 0.3$ . (a), (b) Magnetic structure factor  $S(q)$  for the indicated values of  $\delta$ . Inset of panel (b) uses  $\Delta_q \equiv q_{\max} - \pi$ , where  $q_{\max}$  is the value of  $q$  at which the local maximum of  $S(q)$  near  $q = \pi$  is observed.

#### IV. PHASE SEPARATION, RVB STATES, AND LUTTINGER LIQUID

In Fig. 1(a) the dashed line inside the PS region fix the boundary between two types of phase separation: in one case, the separation occurs between Nagaoka ferromagnetism and short-range RVB states (F-RVB); while in the other, it occurs between IC and short-range RVB states (IC-RVB). Indeed, for  $0 \leq J \lesssim 0.063$  and  $\delta_{F-RVB} \leq \delta < 1/3$ , the GS phase separates with F and short-range RVB states under coexistence, where  $\delta_{F-RVB}$  denotes hole-density values along the phase separation line F-RVB, thereby extending our previous result [13] that was valid only for  $J = 0$ . However, for  $0.063 \lesssim J \leq 0.4$  the system behaves differently. The new PS (IC-RVB) region is here illustrated for  $J = 0.3$ ,  $N = 3N_c + 1 = 100$  sites, and  $N_h = 18$  holes: we thus find that there are 26 cells with odd parity ( $p_l = -1$ ) associated with the IC phase, and the remaining 7 cells with even parity ( $p_l = +1$ ), associated with the RVB phase. In this case, as shown in Fig. 4, the

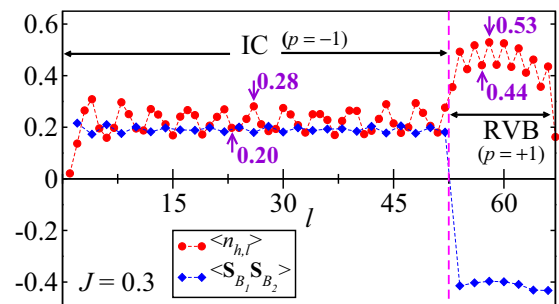


FIG. 4. (Color online) Phase separation (IC-RVB) for a chain with  $N = 3N_c + 1 = 100$  sites,  $J = 0.3$ , and  $N_h = 18$  holes: spin correlation function between  $B$  spins at the same cell,  $\langle \mathbf{S}_{B_1,l} \cdot \mathbf{S}_{B_2,l} \rangle$ , and hole-density profile,  $\langle n_{h,l} \rangle$ .

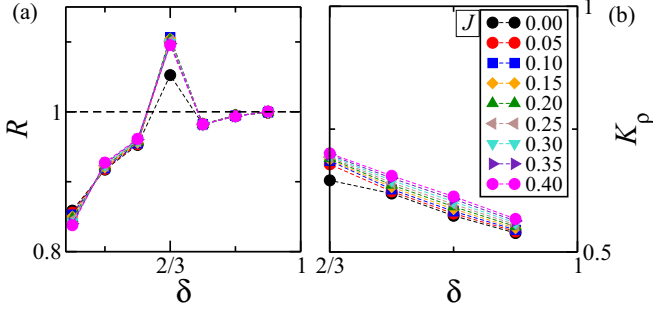


FIG. 5. (Color online) Luttinger liquid behavior for a chain with  $N = 3N_c = 24$  (ED results). (a) Ratio  $R = u_\rho / \sqrt{D\chi/\pi}$  as a function of  $\delta$  for the indicated values of  $J$ . (b) Exponent  $K_\rho$  as a function of  $\delta$ .

hole-poor IC phase presents a local spin correlation function  $\langle \mathbf{S}_{B_1,l} \cdot \mathbf{S}_{B_2,l} \rangle \approx 0.2$ , average hole density per site  $\approx 0.16$ , estimated from the sites indicated by arrows [one  $A$  site and two  $B$  sites in the context of the effective linear chain shown in Fig. 2(a)], and hole-density wave with  $\lambda \approx 4$ ; while the hole-rich RVB phase presents  $\langle \mathbf{S}_{B_1,l} \cdot \mathbf{S}_{B_2,l} \rangle \approx -0.4$  and average hole density per site  $\approx 1/3$ , estimated from a cell with  $A$  and  $B$  sites indicated by arrows. Therefore, apart from boundary effects, the above results thus indicate that the phase separation for a given  $J$  value is defined by the coexistence of the two phases with the hole densities  $\delta_{\text{IC-PS}} (\approx 0.16$  for  $J = 0.3$ ) and  $\delta_{\text{PS-RVB}} (\approx 1/3$  for  $J = 0.3$ ) fixed at the IC-PS and PS-RVB boundaries, respectively, while the size of the phases are fixed by the chemical doping  $\delta = N_h/N$  ( $= 0.18$  for  $N = 100$  and  $N_h = 18$ ). We also remark that the stable RVB phase observed at  $\delta = 1/3$  and  $0 \leq J \leq 0.4$ , which has finite charge and spin gaps, is in agreement with predictions for  $J = 0.35$  [12] and  $J = 0$  [13].

For  $0 \leq J \leq 0.4$  and  $1/3 < \delta < 2/3$ , a crossover region with the presence of long-range RVB states after hole addition away from  $\delta = 1/3$  is observed [see Fig. 1(a)]. At the commensurate filling  $\delta = 2/3$ , the system presents a charge gap, while the spin excitation is gapless, also extending our previous result for  $J = 0$  [13].

With the aim of investigating the LL behavior as a function of  $J$  and  $\delta \geq 2/3$ , we have calculated, through ED techniques, the ratio  $R = u_\rho / \sqrt{D\chi/\pi}$ , where

$$\chi = \frac{N_c}{4} [E(N_h + 2) + E(N_h - 2) - 2E_{\text{GS}}(N_h)] \quad (3)$$

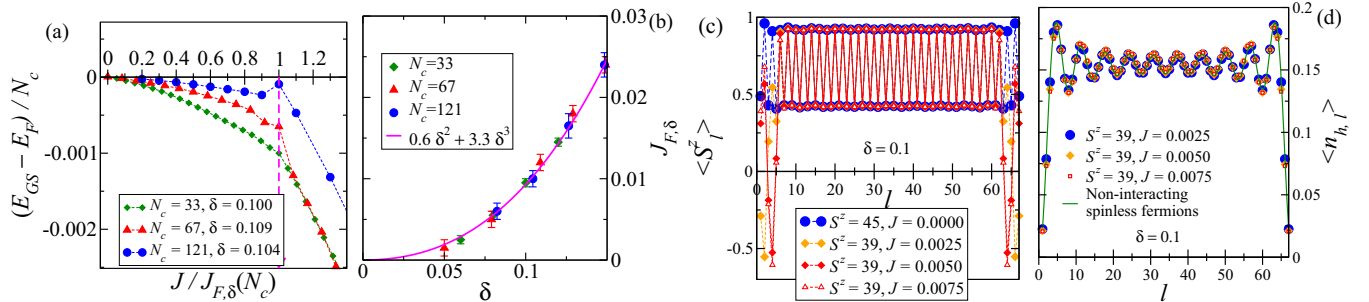


FIG. 6. (Color online) (a) Shift  $E_{\text{GS}} - E_F$  per unit cell, where  $E_F$  is the energy of the fully polarized ferromagnetic state, as a function of  $J/J_{F,\delta}$  for the indicated values of  $N_c$  and  $\delta$ . (b) Instability line of the Nagaoka ferromagnetic phase. (c) Spin and (d) hole profiles,  $\langle n_{h,l} \rangle$  and  $\langle S_l^z \rangle$ , respectively, for a chain with  $N = 3N_c + 1 = 100$ ,  $\delta = 0.1$ , and the indicated values of  $S^z$  and  $J$ .

is the charge susceptibility, and  $E(N_h \pm 2)$  is the total energy for  $N_h \pm 2$  holes;

$$D = \frac{N_c}{4\pi} \left[ \frac{\partial^2 E(\Phi)}{\partial \Phi^2} \right]_{\Phi_{\text{min}}} \quad (4)$$

is the Drude weight, where  $E(\Phi)$  is the lowest energy for a magnetic flux  $\Phi$  through a closed chain, and  $\Phi_{\text{min}}$  is its value at  $E_{\text{GS}}$ ;

$$u_\rho = \frac{E(k_{\text{GS}} + \Delta k, S = 0) - E_{\text{GS}}(k_{\text{GS}}, S_{\text{GS}} = 0)}{\Delta k} \quad (5)$$

is the charge excitation velocity, where  $\Delta k = 2\pi/N_c$ , and  $E(k_{\text{GS}} + \Delta k, S = 0)$  is the lowest energy with wave number  $k = k_{\text{GS}} + \Delta k$  and total spin  $S = S_{\text{GS}} = 0$ . If the low-energy physics of the system is that of a LL, we should find  $R = 1$  [40]; moreover, the exponent governing the asymptotic behavior of the correlation functions,  $K_\rho$ , satisfies the relation  $K_\rho = \pi u_\rho / (2\chi)$ . As shown in Fig. 5(a),  $R$  is indeed very close to 1 for  $\delta > 2/3$ ; in addition, as shown in Fig. 5(b), we find  $0.7 \gtrsim K_\rho \gtrsim 0.5$  for  $\delta > 2/3$ . Remarkably, as shown in Figs. 5(a) and 5(b), the data for  $R$  and  $K_\rho$  exhibit data collapse as a function of  $\delta$  for  $0 \leq J \leq 0.4$ . In short, the results above clearly indicate that, for  $\delta > 2/3$  and  $0 \leq J \leq 0.4$ , the system behaves as a LL in the strong-coupling regime.

## V. STABILITY OF NAGAOKA FERROMAGNETISM

In this section, we provide strong evidence that, for  $0 \leq J \leq J_{F,\delta}$  and  $0 < \delta \leq \delta_{F,\text{RVB}}$ , the kinetic energy of holes is lowered in a fully polarized ferromagnetic state, an extension of Nagaoka ferromagnetism [23,24], with the GS energy equal to that of noninteracting spinless fermions:  $E_{\text{GS}} = E_F$ .

The estimate of  $J_{F,\delta}$  is based on the data for the shift  $(E_{\text{GS}} - E_F)/N_c$  as a function of  $J$ , as illustrated in Fig. 6(a) for  $\delta$  close or equal to 0.1. We stress that the shift decreases as  $N_c$  increases for  $0 < (J/J_{F,\delta}) < 1$  and goes to zero in the thermodynamic limit. In addition, one should notice that, by examining the data above and below  $J = J_{F,\delta}$ , particularly for  $N = 3N_c + 1 = 364$  sites,  $\partial E_{\text{GS}}/\partial J$  appears to be discontinuous at  $J = J_{F,\delta}$  in the thermodynamic limit, thus suggesting a first-order transition to the IC phase at  $(J/J_{F,\delta}) = 1$ . In Fig. 6(b) we show that our estimated transition line,  $J_{F,\delta}$ , [see also Fig. 1(a)] is almost not affected by finite-size effects and implies  $\delta_{F,J} \sim \sqrt{J}$  as  $\delta \rightarrow 0$ , as found from analytical results [27,28] for

the  $t$ - $J$  model in a square lattice. In particular, for  $J = 0$  the instability of the Nagaoka state occurs at  $\delta \approx 0.23$ , which is very close to the values of hole doping estimated for  $n$ -leg ladder systems [25] and the square lattice [25,26].

The spin profile for a chain with  $N = 3N_c + 1 = 100$ ,  $J \gtrsim 0$ , and  $\delta = 0.1$  is also in very good agreement with the Nagaoka state, as shown in Fig. 6(c), although boundary effects are visible for  $J \gtrsim 0$ ; in fact,  $S^z$  changes from 45 to 39 (on average, three spins at each boundary are not fully polarized), but one should notice that the change saturates as  $J$  slightly increases above zero. This fact is corroborated by the hole density shown in Fig. 6(d), whose data for the referred states with  $S^z = 39$  at  $\delta = 0.1$  are very well described by the Nagaoka profile.

## VI. DISCUSSION AND CONCLUDING REMARKS

The presented phase diagram of doped  $AB_2$   $t$ - $J$  chains is remarkably rich. Indeed, several magnetic and nonmagnetic

phases manifest themselves in a succession of surprising relevant features, some of which are similar to those observed in the square and  $n$ -leg ladder lattices: all in a simple doped chain. In particular, we emphasize the modulated ferrimagnetic structure, the occurrence of Nagaoka spin polarons in the underdoped regime and small values of  $J$ , incommensurate structures with nonzero magnetization, the strong-coupling LL physics in the high-doped regime, and the instability of Nagaoka ferromagnetism against  $J$  and doping. Therefore, these chains are unique systems and of relevance for the physics of polymeric materials, whose properties might also represent challenging topics to be explored via analog simulations in ultracold fermionic optical lattices.

## ACKNOWLEDGMENTS

This work was supported by CNPq and FACEPE through the PRONEX program, and CAPES (Brazilian agencies).

- 
- [1] *The Hubbard Model—A Reprint Volume*, edited by A. Montorsi (World Scientific, Singapore, 1992).
- [2] F. Gebhard, *The Mott Metal-Insulator Transition* (Springer, Berlin, 1997); M. Imada, A. Fujimori, and Y. Tokura, *Rev. Mod. Phys.* **70**, 1039 (1998).
- [3] A. Auerbach, *Interacting Electrons and Quantum Magnetism* (Springer, Berlin, 1998).
- [4] P. W. Anderson, *Science* **235**, 1196 (1987); *The Theory of Superconductivity in the High- $T_c$  Cuprates* (Princeton University Press, Princeton, 1997); P. A. Lee, N. Nagaosa, and X.-G. Wen, *Rev. Mod. Phys.* **78**, 17 (2006).
- [5] E. H. Lieb and F. Y. Wu, *Phys. Rev. Lett.* **20**, 1445 (1968); F. H. L. Essler, H. Frahm, F. Gohmann, A. Klumper, and V. E. Korepin, *The One-Dimensional Hubbard Model* (Cambridge University Press, Cambridge, 2005).
- [6] E. H. Lieb, in *The Hubbard Model, Its Physics and Mathematical Physics*, Nato ASI, Series B: Physics, edited by D. Baeriswyl, D. K. Campbell, J. M. P. Carmelo, F. Guinea, and E. Louis, Vol. 343 (Plenum, New York, 1995); H. Tasaki, *J. Phys.: Condens. Matter* **10**, 4353 (1998); G.-S. Tian, *J. Stat. Phys.* **116**, 629 (2004).
- [7] E. H. Lieb, *Phys. Rev. Lett.* **62**, 1201 (1989).
- [8] E. Lieb and D. Mattis, *J. Math. Phys.* **3**, 749 (1962).
- [9] A. M. S. Macêdo, M. C. dos Santos, M. D. Coutinho-Filho, and C. A. Macêdo, *Phys. Rev. Lett.* **74**, 1851 (1995).
- [10] G.-S. Tian and T.-H. Lin, *Phys. Rev. B* **53**, 8196 (1996).
- [11] S.-D. Liang, Z. D. Wang, Q. Wang, and S.-Q. Shen, *Phys. Rev. B* **59**, 3321 (1999).
- [12] G. Sierra, M. A. Martín-Delgado, S. R. White, D. J. Scalapino, and J. Dukelsky, *Phys. Rev. B* **59**, 7973 (1999); M. A. Martín-Delgado, J. Rodríguez-Laguna, and G. Sierra, *ibid.* **72**, 104435 (2005).
- [13] R. R. Montenegro-Filho and M. D. Coutinho-Filho, *Phys. Rev. B* **74**, 125117 (2006); M. H. Oliveira, E. P. Raposo, and M. D. Coutinho-Filho, *ibid.* **80**, 205119 (2009).
- [14] A. A. Lopes and R. G. Dias, *Phys. Rev. B* **84**, 085124 (2011); A. A. Lopes, B. A. Z. António, and R. G. Dias, *ibid.* **89**, 235418 (2014).
- [15] For Bose-Hubbard models, see J. J. García-Ripoll and J. K. Pachos, *New J. Phys.* **9**, 139 (2007); S. Takayoshi, H. Katsura, N. Watanabe, and H. Aoki, *Phys. Rev. A* **88**, 063613 (2013).
- [16] E. P. Raposo and M. D. Coutinho-Filho, *Phys. Rev. Lett.* **78**, 4853 (1997); *Phys. Rev. B* **59**, 14384 (1999); C. Vitoriano, M. D. Coutinho-Filho, and E. P. Raposo, *J. Phys. A: Math. Gen.* **35**, 9049 (2002).
- [17] F. C. Alcaraz and A. L. Malvezzi, *J. Phys. A: Math. Gen.* **30**, 767 (1997).
- [18] R. R. Montenegro-Filho and M. D. Coutinho-Filho, *Physica A (Amsterdam, Neth.)* **357**, 173 (2005); S. Yamamoto and J. Ohara, *Phys. Rev. B* **76**, 014409 (2007).
- [19] N. Ivanov, *Condens. Matter Phys.* **12**, 435 (2009).
- [20] R. R. Montenegro-Filho and M. D. Coutinho-Filho, *Phys. Rev. B* **78**, 014418 (2008); K. Hida and K. Takano, *ibid.* **78**, 064407 (2008); A. S. F. Tenório, R. R. Montenegro-Filho, and M. D. Coutinho-Filho, *ibid.* **80**, 054409 (2009); T. Shimokawa and H. Nakano, *J. Phys. Soc. Jpn.* **81**, 084710 (2012); S. C. Furuya and T. Giamarchi, *Phys. Rev. B* **89**, 205131 (2014).
- [21] M. S. S. Pereira, F. A. B. F. de Moura, and M. L. Lyra, *Phys. Rev. B* **77**, 024402 (2008); **79**, 054427 (2009); O. Rojas, S. M. de Souza, and N. S. Ananikian, *Phys. Rev. E* **85**, 061123 (2012).
- [22] M. D. Coutinho-Filho, R. R. Montenegro-Filho, E. P. Raposo, C. Vitoriano, and M. H. Oliveira, *J. Braz. Chem. Soc.* **19**, 232 (2008).
- [23] Y. Nagaoka, *Phys. Rev.* **147**, 392 (1966).
- [24] H. Tasaki, *Prog. Theor. Phys.* **99**, 489 (1998).
- [25] L. Liu, H. Yao, E. Berg, S. R. White, and S. A. Kivelson, *Phys. Rev. Lett.* **108**, 126406 (2012).
- [26] F. Becca and S. Sorella, *Phys. Rev. Lett.* **86**, 3396 (2001).
- [27] E. Eisenberg, R. Berkovits, David A. Huse, and B. L. Altshuler, *Phys. Rev. B* **65**, 134437 (2002).
- [28] M. M. Maška, M. Mierzejewski, E. A. Kochetov, L. Vidmar, J. Bonča, and O. P. Sushkov, *Phys. Rev. B* **85**, 245113 (2012).
- [29] E. Dagotto, *Science* **309**, 257 (2005).
- [30] S. Chakrabarty, V. Dobrosavljević, A. Seidel, and Z. Nussinov, *Phys. Rev. E* **86**, 041132 (2012).

- [31] J. M. Tranquada, *Physica B (Amsterdam, Neth.)* **407**, 1771 (2012).
- [32] V. J. Emery, S. A. Kivelson, and H. Q. Lin, *Phys. Rev. Lett.* **64**, 475 (1990).
- [33] P. Corboz, S. R. White, G. Vidal, and M. Troyer, *Phys. Rev. B* **84**, 041108 (2011).
- [34] W.-J. Hu, F. Becca, and S. Sorella, *Phys. Rev. B* **85**, 081110 (2012).
- [35] P. Corboz, T. M. Rice, and M. Troyer, *Phys. Rev. Lett.* **113**, 046402 (2014).
- [36] M. Ogata, M. U. Luchini, S. Sorella, and F. F. Assaad, *Phys. Rev. Lett.* **66**, 2388 (1991).
- [37] S. R. White, *Phys. Rev. B* **48**, 10345 (1993); U. Schollwöck, *Rev. Mod. Phys.* **77**, 259 (2005).
- [38] F. D. M. Haldane, *J. Phys. C* **14**, 2585 (1981); J. Voit, *Rep. Prog. Phys.* **58**, 977 (1995); T. Giamarchi, *Quantum Physics in One Dimension* (Oxford University Press, New York, 2003).
- [39] A. Auerbach and B. E. Larson, *Phys. Rev. Lett.* **66**, 2262 (1991); E. Dagotto and J. R. Schrieffer, *Phys. Rev. B* **43**, 8705 (1991).
- [40] See, e.g., C. A. Hayward and D. Poilblanc, *Phys. Rev. B* **53**, 11721 (1996).